

Supplementary Information

Alcohol-induced Decomposition of Olmstead's Crystalline Ag(I)- Fullerene Heteronanostructure yields 'Bucky Cubes'

Lok Kumar Shrestha, Marappan Sathish, Jonathan P. Hill, Kun'ichi Miyazawa, Tohru Tsuruoka,
Noelia Sanchez-Ballester, Itaru Honma, Qingmin Ji and Katsuhiko Ariga

Contents:

1. Focused ion beam cutting of bucky cubes	S8
2. Additional SEM images	S10
3. Bucky cube interiors.....	S11
4. Differing transformations at crystal planes	S13
5. Electron diffraction of C ₆₀ whisker crystals.....	S14
6. Photoluminescence spectra of cubes.....	S15
7. X-ray powder diffraction of bucky cubes and reduced bucky cubes	S17

1. Additional imaging of focused ion beam cutting of bucky cubes.

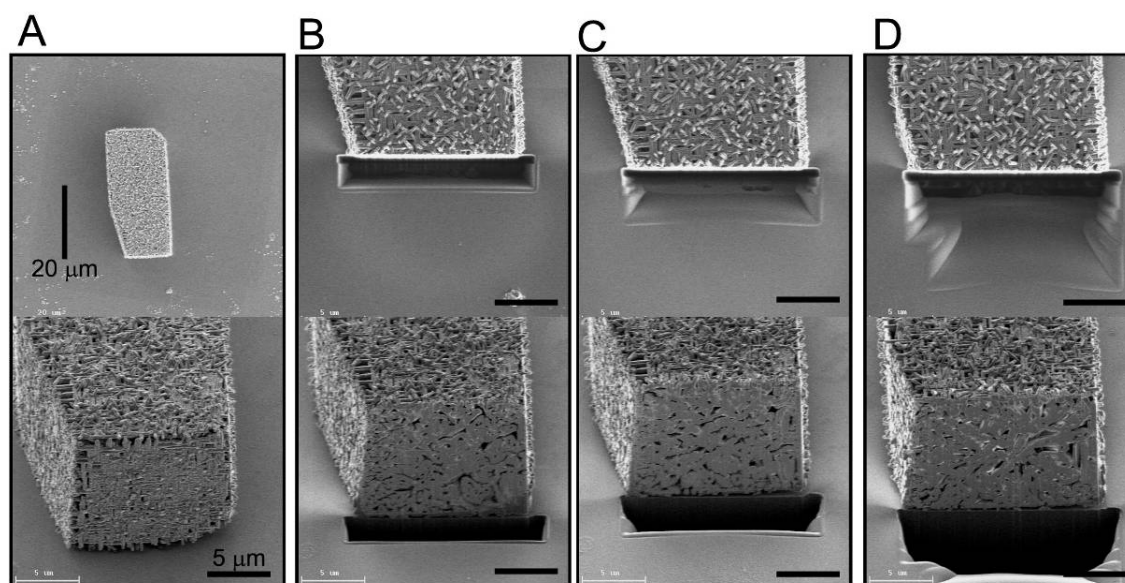


Figure S1. Similar sectioning as shown in Figure 6 of the manuscript. (A) Starting point. (B) 2 μm. (C) 4 μm. (D) 10 μm. Even at 10 μm depth transformation to the fullerene microcrystalline state has occurred. Lower panels of each figure show a 45° elevation of the cut cube surface.

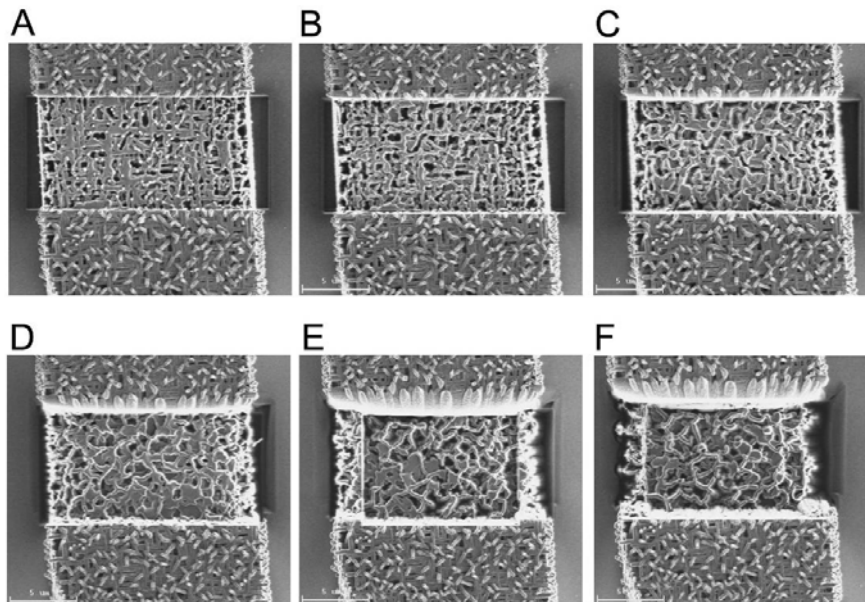


Figure S2. FIB section through the center of a bucky cube at depth (A) 1 μm. (B) 2 μm. (C) 4.5 μm. (D) 5 μm. (E) 7 μm. (F) 11 μm. Note that bucky cube morphology at the cutting site becomes distressed although it is clearly not homogenous as expected for pristine crystals of $C_{60}\{AgNO_3\}_5$ (see Figure S3).

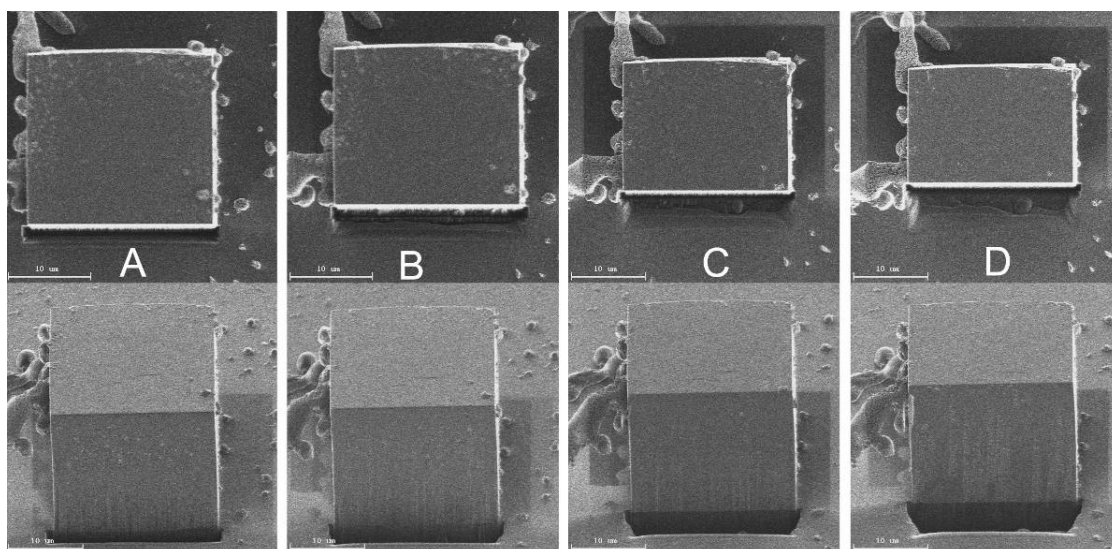


Figure S3. FIB section through a freshly prepared crystal of $C_{60}\{AgNO_3\}_5$ revealing its excellent homogeneity and lack of microstructure at the interior.

2. Additional SEM images.

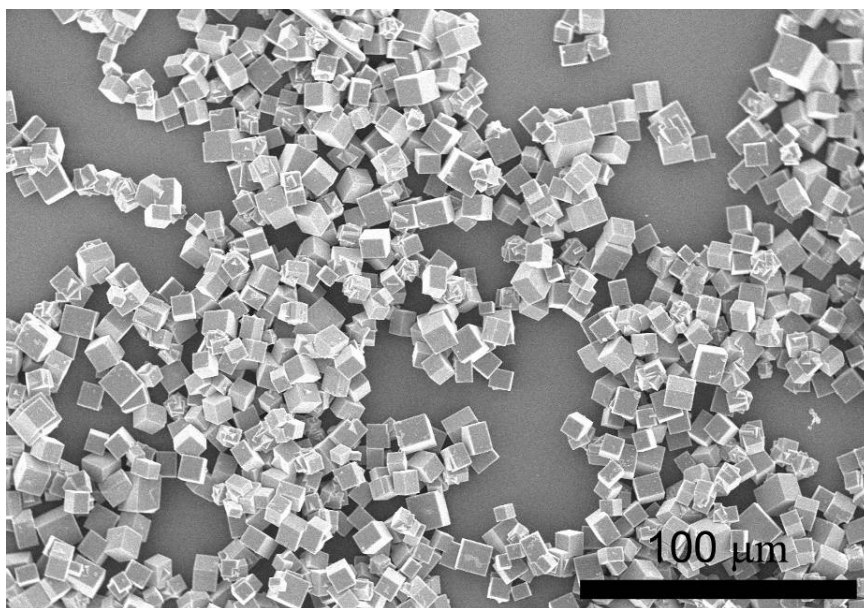


Figure S4. SEM image of microcrystalline sample of $C_{60}\{AgNO_3\}_5$.

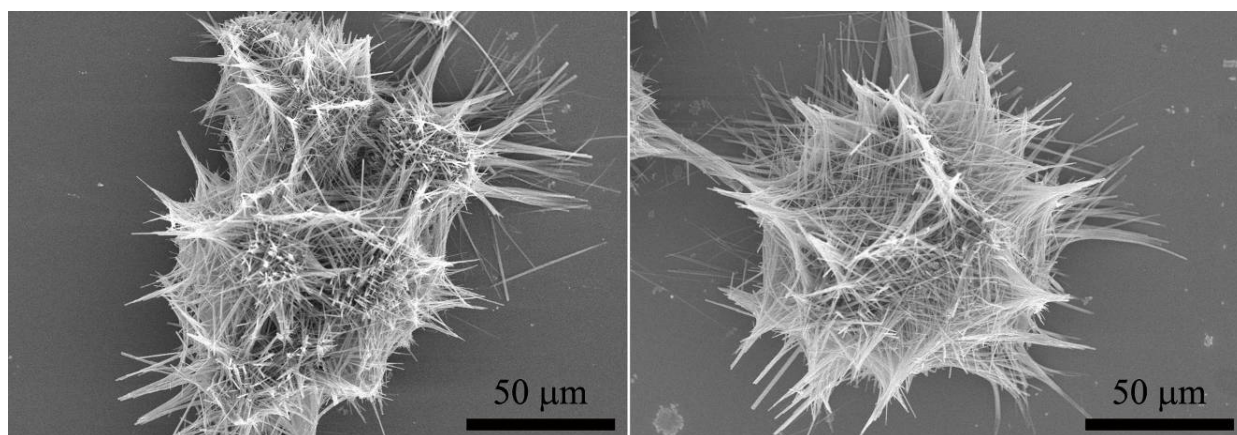


Figure S5. SEM image of bucky cubes that have been washed consecutively with 1-butanol. Note that cube morphology has almost been lost and whisker-like crystals grow at random.

3. Bucky cube interiors.

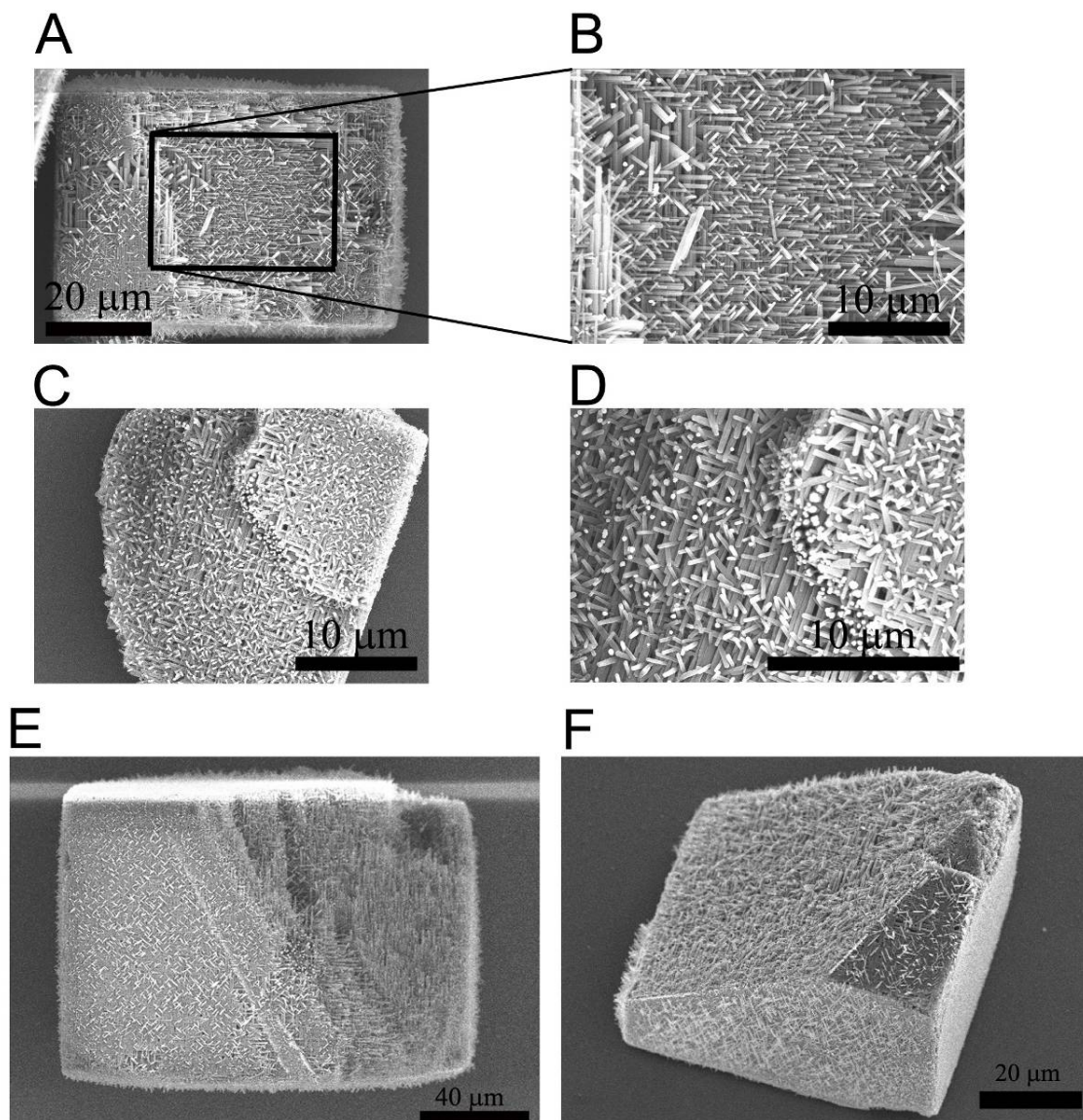


Figure S6. Interiors of adventitiously broken bucky cubes revealing the interior structure. (A),(B) Single cube exhibits highly structured formation at its interior after breaking. (C) Fragment of a bucky cube and (D) an a magnified view. (E) Bucky cube interior that contains a forest of C₆₀ whiskers. (F) A further example of structuring in a compromised bucky cube.

4. Differing transformations at crystal planes.

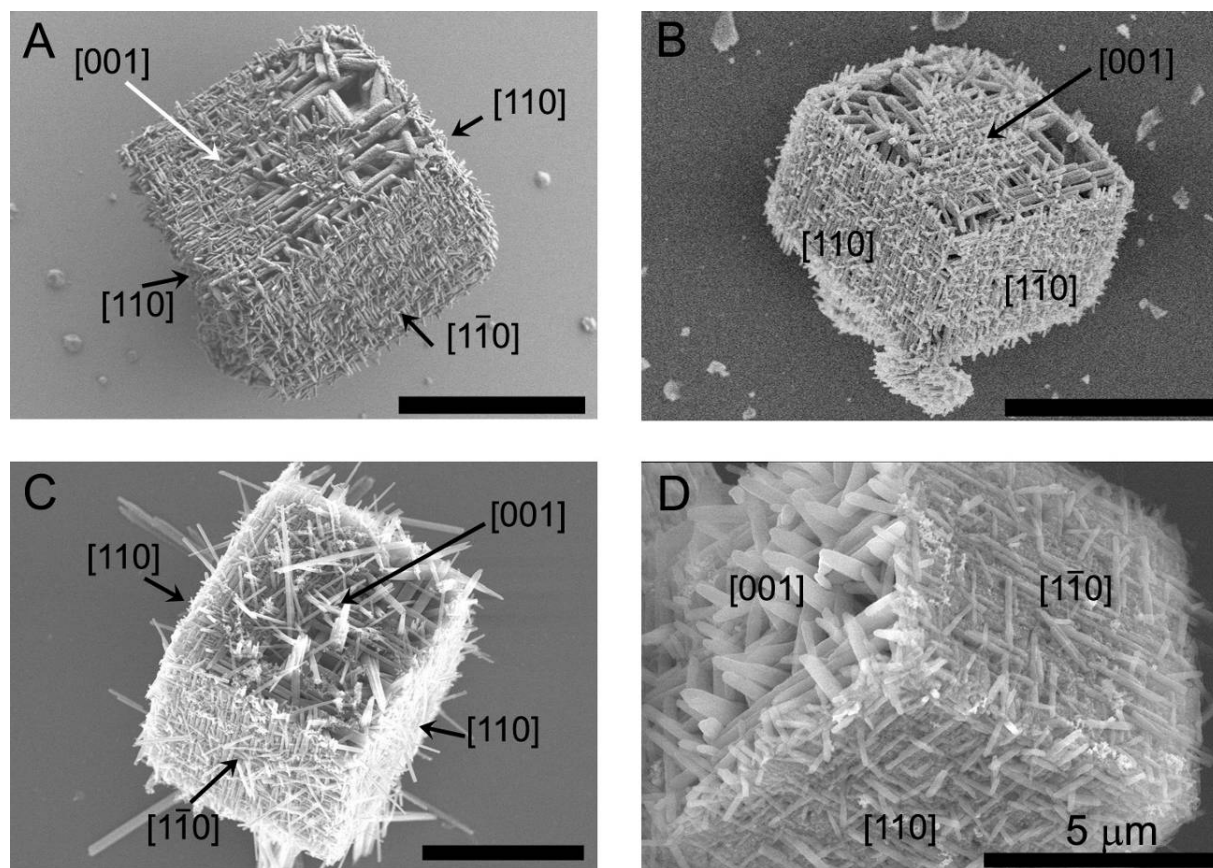


Figure S7. (A)-(D) Occasionally observed SEM images of bucky cubes indicating different transformation properties at different faces of the starting material. Suggested crystal face assignments corresponding to the starting material are given.

5. Electron diffraction of C_{60} whisker crystals.

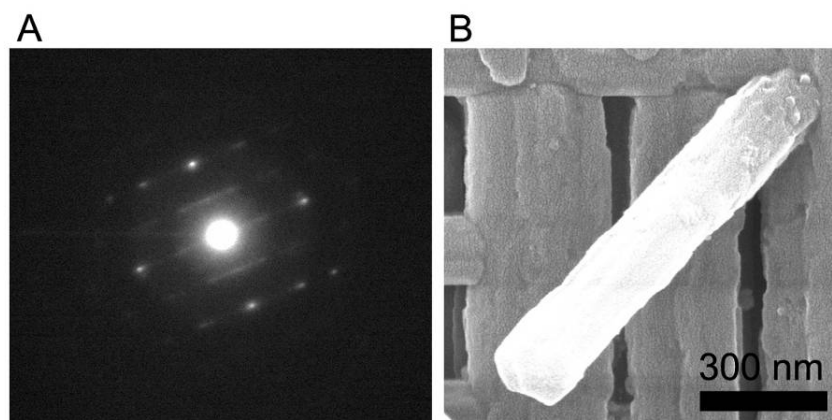


Figure S8. (A) Typical electron diffraction image of a single C_{60} whisker microcrystal contained in the bucky cubes. (B) A crystal of C_{60} grown at the face of a bucky cube. These whiskers are typically 100 – 200 nm in diameter.

6. Photoluminescence spectra of cubes.

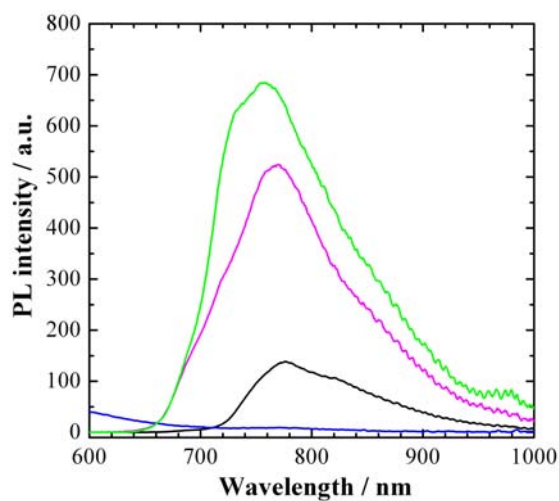


Figure S9. Photoluminescence (PL) spectra excited at 514.5 nm of C_{60} powder (black line), $C_{60}\{AgNO_3\}_5$ (blue line), bucky cubes (pink line) and C_{60} 1-D nanorods (green line).

7. X-ray powder diffraction of bucky cubes and reduced bucky cubes

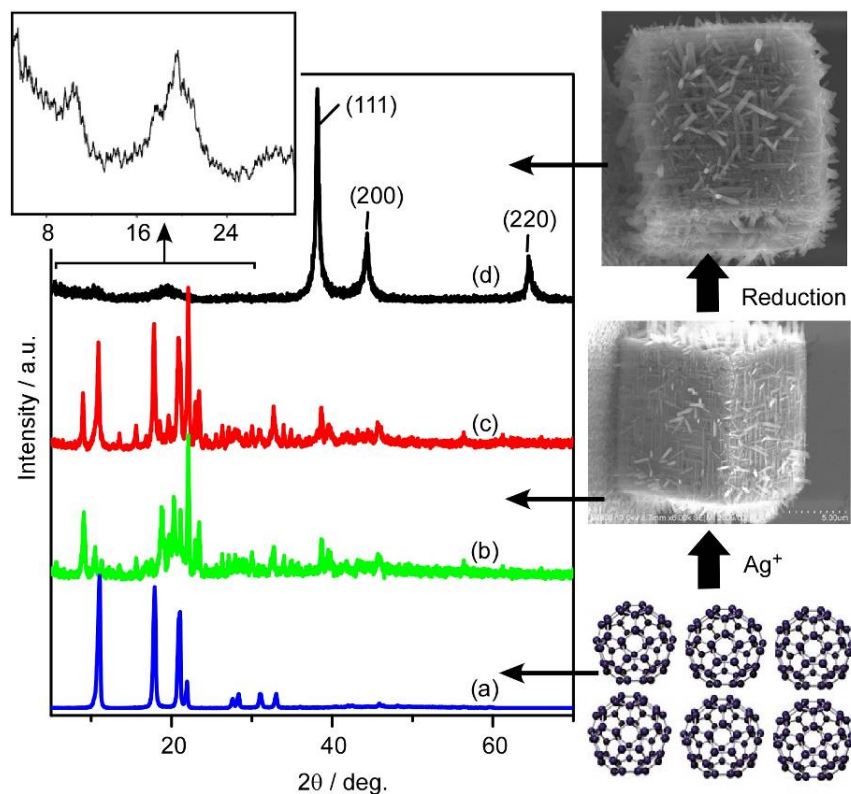


Figure S10. XRD patterns. **a**, C₆₀ powder with the fcc crystalline structure. **b**, bucky cubes. **c**, bucky cubes after drying at 150 °C in vacuum. **d**, bucky cubes containing fcc crystalline metallic Ag [(100), (200) and (220) peaks due to elemental silver are clear] after reduction using hydrazine monohydrate. Inset indicates crystallinity of the C₆₀ component.